Progress In Electromagnetics Research B, Vol. 56, 219–234, 2013

DIRECTION FINDING IN THE PRESENCE OF NEAR ZONE RESONANT SIZE SCATTERERS

Irfan Ahmed[1, 2, *] and Warren Perger[2]

[1]Department of Electronic Engineering, NED University of Engineering & Technology, University Road, Karachi 75270, Pakistan

[2]Department of Electrical and Computer Engineering, Michigan Technological University, 1400 Townsend Drive Houghton, MI 49931, USA

Abstract—A self calibration algorithm for direction finding in the presence of arbitrary shape 3D scatterers of resonating size is presented. This algorithm removes the effects of mutual coupling and 3D scatterers on direction of arrival estimation. The scatterers and wire type antenna array are excited by incident plane waves of arbitrary direction. The 3D scatterers shape is approximated as a sphere, thus spherical harmonics are assumed to be originated in response to the plane wave excitation. The algorithm requires the location of the scatterers with reference to antenna elements. However, knowledge of exact shape of scatterers is not required. Moreover, scatterers may be located in near or far fields. The work is supported by numerical examples for different scenarios of multiple incident waves and scatterers.

1. INTRODUCTION

Wireless devices with the capability of direction-of-arrival estimation (DOA) have many applications such as command and control, security and safety and MIMO communication. Several techniques have been developed and presented in the literature to estimate DOA [1]. More recently, a DOA estimation technique which does not require subspace decomposition is also presented [2]. In general these methods assume that the antenna elements are ideal and operate in free space. The real-world problem is totally different where antenna elements share energy

Received 30 May 2013, Accepted 30 October 2013, Scheduled 1 November 2013

* Corresponding author: Irfan Ahmed (iahmed@mtu.edu).

with themselves, known as mutual coupling. Moreover the presence of scatterers in the vicinity of antenna results in distortion of the signal and causes DOA estimation error [3].

A number of researchers proposed methods to compensate for the effects of mutual coupling for real antenna elements [4–10]. These techniques proved effective in significant reduction of errors in DOA estimation for an array operating in an environment similar to free space. Thus the presence of any near zone scatterer is ignored or not considered in the signal model. These methods also assume that sources are in the far field and therefore incident waves are plane waves. However any scatterer in the near zone produces spherical waves, when illuminated by far field sources [11]. The plane waves from the far field are desired signals, and spherical waves due to near-zone scattering are the interfering signals.

In the last decade some authors addressed the joint problem of mutual coupling and near-zone scatterers, by techniques whose essence is offline calibration [3, 12, 13]. Fewer antenna elements are required by transforming the non-uniform array to a virtual uniform array to find DOA in an environment for which steering vectors are previously measured/computed [3]. Non-conventional least square optimization is used to exploit the large data set of pre-calibrated steering vectors for DOA estimation with near zone scatterers [12]. The square calibration matrix of [6] is proposed as non-square to address the scattering from a known scatterer or platform structure [13]. These methods are suitable for fixed antenna where the environment remain stationary. However when either antenna is portable or environment is not stationary, these methods will yield errors and require re-calibration, which is not convenient for many applications.

One way to address the issue of portable antenna where pre-calibration cannot last long is self- or auto-calibration. The auto-calibration techniques exploit the signals from the sources of opportunity to sufficiently remove errors in the DOA estimate, while estimating the DOA simultaneously. Thus no additional source is required to calibrate the array. A self-calibration technique for DOA estimation using MUSIC algorithm where an uncoupled near-field scatterer is present is in the literature [11]. This method does not remove the effects of mutual coupling and works only for 2D scatterers. A self calibration algorithm that removes the effects of mutual coupling and near zone scatterer is also in the literature [14]. This algorithm approximates a scatterer as a cylinder, and therefore assumes cylindrical harmonic expansion origination in response to a plane wave incidence. The algorithm is iterative and does not guarantee the achievement of the true DOA but rather convergence.

It also works only for 2D scatterers and requires a large number of antenna elements.

In a real-world 3D environment, a finite-size scatterer is more accurately modeled as a sphere, and as stated by [11] produces spherical harmonics in response to plane wave excitation. This paper extends the iterative algorithm approach presented in [14] to a 3D case where scatterers are modeled as a sphere and the algorithm utilizes spherical harmonic expansion. Although as its predecessor, a solution is not guaranteed but convergence is achieved with far less number of antenna elements. It is highly likely that the presence of near-zone scatterers results in spurious peaks in the DOA spectrum, which cause errors in the initial estimate of the number of sources [12, Figure 14]. This issue of spurious number of sources was not explicitly described in [14]. Our algorithm suppresses the spurious peaks and corrects the detection of number of sources, in addition to the removal of DOA estimation errors. Classical DOA estimation methods [15, 16] are incorporated in this algorithm. The algorithm estimates elevation θ_l of incident sources present in the far field.

Section 2 will describe the method and explain the algorithm. Numerical examples showing capability of the method for a variety of complexities are presented in Section 3. Section 4 concludes the paper. An Appendix provides symbol definitions and nomenclature.

2. METHOD DESCRIPTION

2.1. Problem Statement

To illustrate the problem, consider TM_x plane waves incident on an antenna array of x-directed thin wires. All currents and fields in antenna elements are also x-directed. Figure 1 shows the problem setup, where a field is incident on an antenna array of M elements, the location of mth element is $\mathbf{r}_m = (x_m, y_m, z_m)$. The scatterers location $\mathbf{r}_s = (x_s, y_s, z_s)$ is known, but geometry is unknown. It is also assumed that the antenna and environment is stationary during DOA estimation.

The total field at the mth antenna element is given as the sum of incident and scattered field (from spherical scatterer)

$$\mathbf{E}^t = \mathbf{E}^{inc} + \mathbf{E}^{sct} \tag{1}$$

The x-directed incident field at the mth antenna element due to

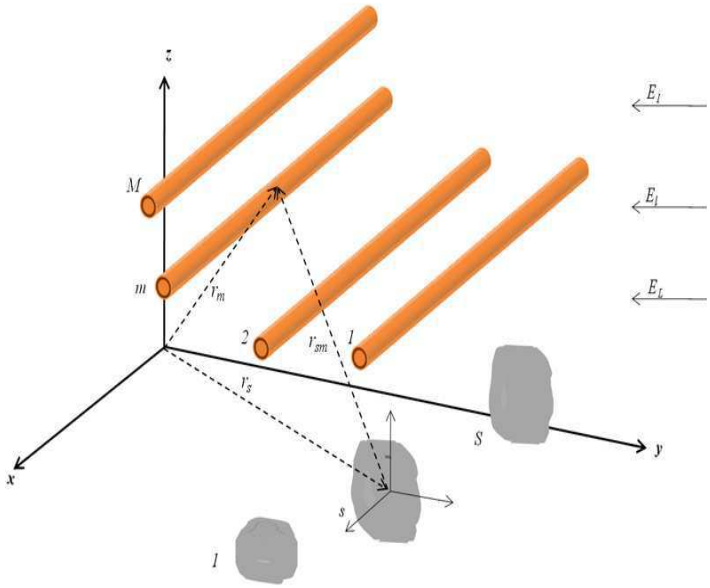

Figure 1. Incident plane wave on M element array with spherical scatterer.

L incident waves is given as

$$E_m^{inc}(x) = \sum_{l=1}^{L} E_l E_m^{PW}(\theta_l, \phi_l)$$
$$= \sum_{l=1}^{L} E_l e^{j\beta(x_m \sin\theta_l \cos\phi_l + y_m \sin\theta_l \sin\phi_l + z_m \cos\theta_l)} \left| E_m^{inc}(x) \right| \quad (2)$$

When a sphere is excited by a TM_x plane wave, the corresponding spherical harmonic expansion is in [17]. Letting the magnitude $|E_m^{inc}(x)| = E_o$, the scattered field along x-axis at mth antenna element due to S spherical scatterers at known location in near zone is given as

$$E_m^{sct}(x) = \sum_{s=1}^{S} \left[(\sin\theta_{sm} \cos\phi_{sm}) \left[-jE_o \cos\phi_{sm} \sum_{q=1}^{\infty} b_{sq} \left[\hat{H}_{sq}^{(2)''}(\beta r_{sm}) + \hat{H}_{sq}^{(2)}(\beta r_{sm}) \right] \right. \right.$$
$$P_{sq}^{1}(\cos\theta_{sm}) \Big] + (\cos\theta_{sm} \cos\phi_{sm}) \left[\frac{E_o}{\beta r_{sm}} \cos\phi_{sm} \sum_{q=1}^{\infty} \left[j b_{sq} \hat{H}_{sq}^{(2)'}(\beta r_{sm}) \right. \right.$$
$$\left. \left. \sin\theta_{sm} P_{sq}^{'1}(\cos\theta_{sm}) - c_{sq} \hat{H}_{sq}^{(2)}(\beta r_{sm}) \frac{P_{sq}^{1}(\cos\theta_{sm})}{\sin\theta_{sm}} \right] \right] + (-\sin\phi_{sm})$$

$$\left[\frac{E_o}{\beta r_{sm}}\sin\phi_{sm}\sum_{q=1}^{\infty}\left[jb_{sq}\hat{H}_{sq}^{(2)'}(\beta r_{sm})\frac{P_{sq}^{1}(\cos\theta_{sm})}{\sin\theta_{sm}}\right.\right.$$
$$\left.\left.-c_{sq}\hat{H}_{sq}^{(2)}(\beta r_{sm})\sin\theta_{sm}P_{sq}^{'1}(\cos\theta_{sm})\right]\right]. \quad (3)$$

To make the equation concise, the following constants can be introduced for a fixed geometrical location

$$U_{sm} = -j\sin\theta_{sm}\cos^2\phi_{sm} \quad (4)$$
$$V_{sm} = \frac{\cos\theta_{sm}\cos^2\phi_{sm}}{\beta r_{sm}} \quad (5)$$
$$W_{sm} = \frac{-\sin^2\phi_{sm}}{\beta r_{sm}}. \quad (6)$$

The individual estimation of source amplitude E_o that excited the scatterers is not our concern so we merged it with unknown amplitudes of the harmonics to form two new unknown amplitudes as following

$$B_{sq} = E_o b_{sq} \quad (7)$$
$$C_{sq} = E_o c_{sq} \quad (8)$$

The five harmonic forms (indexed in superscript) can be written as

$$G_{sqm}^{1} = \left[\hat{H}_{sq}^{(2)''}(\beta r_{sm}) + \hat{H}_{sq}^{(2)}(\beta r_{sm})\right]P_{sq}^{1}(\cos\theta_{sm}) \quad (9)$$
$$G_{sqm}^{2} = j\hat{H}_{sq}^{(2)'}(\beta r_{sm})\sin\theta_{sm}P_{sq}^{'1}(\cos\theta_{sm}) \quad (10)$$
$$G_{sqm}^{3} = \hat{H}_{sq}^{(2)}(\beta r_{sm})\frac{P_{sq}^{1}(\cos\theta_{sm})}{\sin\theta_{sm}} \quad (11)$$
$$G_{sqm}^{4} = j\hat{H}_{sq}^{(2)'}(\beta r_{sm})\frac{P_{sq}^{1}(\cos\theta_{sm})}{\sin\theta_{sm}} \quad (12)$$
$$G_{sqm}^{5} = \hat{H}_{sq}^{(2)}(\beta r_{sm})\sin\theta_{sm}P_{sq}^{'1}(\cos\theta_{sm}) \quad (13)$$

Therefore Equation (3) can be simplified in the form of known harmonics and their unknown amplitudes as following:

$$E_m^{sct}(x) = \sum_{s=1}^{S}\left[U_{sm}\sum_{q=1}^{Q}B_{sq}G_{sqm}^{1} + V_{sm}\sum_{q=1}^{Q}\left[B_{sq}G_{sqm}^{2} - C_{sq}G_{sqm}^{3}\right]\right.$$
$$\left.+W_{sm}\sum_{q=1}^{Q}\left[B_{sq}G_{sqm}^{4} - C_{sq}G_{sqm}^{5}\right]\right]. \quad (14)$$

Note that we are not determining the current density on the scatterer as it is not needed for our method. Suppose our receiver is capable of measuring total voltage at mth antenna terminal V_m^t. The total voltage received at an antenna terminal can be expressed as following:

$$V_m^t = V_m^{inc} + V_m^{sct} \tag{15}$$

where at the mth antenna terminal V_m^{inc} is the voltage due to the incident filed $E_m^{inc}(x)$ alone and V_m^{sct} is the voltage due to scattered field arising from near-zone scatterers $E_m^{sct}(x)$.

2.2. Solution

As mentioned earlier, the total voltage at the antenna terminal is measured or known. The iterative technique to determine DOA by finding V^{inc} and V^{sct} from the knowledge of V^t is described here. The algorithm removes the effects of mutual coupling in an implicit way by forcing V^{inc} as coupling free voltage vector, while putting all the perturbations in V^{sct} vector. In the absence of any scatterer, the environment can be considered as free space and V_m^t suffers perturbation due to mutual coupling between elements only. In this special case ($S = 0$) any of the available methods [4–8, 10] can be embedded along this proposed iterative algorithm. The index of iteration $k = 0, 1, 2, \ldots, K$ is used in superscript of unknown parameters described in previous section. At convergence the iteration index is noted as K. The following steps describe the algorithm:

(i) Given the V^t is known and initially assumed as the desired V^{inc} voltage, and classical DOA estimation techniques are also available [16, 18]. At $k = 0$ the iteration estimates number of sources $L^{(k)}$ and their elevation $\theta = [\theta_1^{(k)}, \theta_2^{(k)}, \ldots, \theta_L^{(k)}])$. It is to be noted that the incorrect assumption of letting $V^t = V^{inc}$ not only causes errors in DOA estimate but may also gives rise to spurious peaks in DOA spectrum [12]. Thus the initial estimate of number of sources may be higher than actual.

(ii) Having number of sources and DOA estimates from step 1, for an array of M elements (15) can be written as set of M simultaneous

linear equations.

$$\begin{bmatrix} V_1^t \\ V_2^t \\ \vdots \\ V_m^t \\ \vdots \\ V_M^t \end{bmatrix} = \begin{bmatrix} \sum_{l=1}^{L} E_1^{PW}(\theta_l,\phi_l) & \sum_{s=1}^{S}\sum_{q=1}^{Q}\left[U_{s1}G_{sq1}^1 + V_{s1}G_{sq1}^2 + W_{s1}G_{sq1}^4\right] \\ \sum_{l=1}^{L} E_2^{PW}(\theta_l,\phi_l) & \sum_{s=1}^{S}\sum_{q=1}^{Q}\left[U_{s2}G_{sq2}^1 + V_{s2}G_{sq2}^2 + W_{s2}G_{sq2}^4\right] \\ \vdots & \\ \sum_{l=1}^{L} E_m^{PW}(\theta_l,\phi_l) & \sum_{s=1}^{S}\sum_{q=1}^{Q}\left[U_{sm}G_{sqm}^1 + V_{sm}G_{sqm}^2 + W_{sm}G_{sqm}^4\right] \\ \vdots & \\ \sum_{l=1}^{L} E_M^{PW}(\theta_l,\phi_l) & \sum_{s=1}^{S}\sum_{q=1}^{Q}\left[U_{sM}G_{sqM}^1 + V_{sM}G_{sqM}^2 + W_{sM}G_{sqM}^4\right] \end{bmatrix} \begin{bmatrix} \sum_{s=1}^{S}\sum_{q=1}^{Q}\left[-V_{s1}G_{sq1}^3 - W_{s1}G_{sq1}^5\right] \\ \sum_{s=1}^{S}\sum_{q=1}^{Q}\left[-V_{s2}G_{sq2}^3 - W_{s2}G_{sq2}^5\right] \\ \sum_{s=1}^{S}\sum_{q=1}^{Q}\left[-V_{sm}G_{sqm}^3 - W_{sm}G_{sqm}^5\right] \\ \sum_{s=1}^{S}\sum_{q=1}^{Q}\left[-V_{sM}G_{sqM}^3 - W_{sM}G_{sqM}^5\right] \end{bmatrix} \begin{bmatrix} E_l^{(k)} \\ B_{sq}^{(k)} \\ C_{sq}^{(k)} \end{bmatrix} \tag{16}$$

We are assuming that scatterers are exterior to the array elements and each scatterer is approximated as a sphere whose radius is ρ_s. The number of harmonics required to sufficiently represent the scattered field from a near zone scatterer can be approximately given as $Q = \beta r_s$. Equal number of harmonics for each scatterer is also assumed for simplicity. Here the unknowns are $E_l^{(k)}$, $B_{sq}^{(k)}$ and $C_{sq}^{(k)}$ where $l = 1, 2, \ldots, L(k)$, $s = 1, 2, \ldots, S$ and $q = 1, 2, \ldots, Q$. Thus the total number of unknowns in above equation is given as $N = L^{(k)} + SQ + SQ = L^{(k)} + 2SQ$. As its predecessor [14], we solve Equation (16) by least square method with condition that $N < M$.

(iii) The incident voltage in each iteration is evaluated as

$$V^{inc} = V^t - V^{sct} \tag{17}$$

where V^{sct} is found through Equation (14) for each antenna by using current values of B & C, the spherical harmonic's amplitudes.

(iv) The incident voltage from above step is used to find elevation of incident sources and iteration index is incremented and algorithm is repeated until convergence of DOA estimate is achieved.

Although there is no surety of achieving the true value or exact DOA but rather convergence is guaranteed. In next section the capability of the method is demonstrated by numerical examples.

3. RESULTS AND DISCUSSION

The examples presented in this section test the algorithm for variety of situations. All examples use horizontal (x-directed) half wave dipoles of wire radius $\rho_a = 0.001\lambda$ as elements of a uniform linear array. The array principal axis is along z direction and its first element center is (0, 0, 0). Examples 1 & 2 have element spacing $d = 0.5\lambda$ and examples 3 & 4 have closely spaced elements with spacing $d = 0.25\lambda$. These examples take into account the more practical radius of antenna element as compared to [14], where it was $\rho_a = 0.00001\lambda$. For example at $f = 3\,\text{GHz}$, our antenna radius will be 1 mm, where further reduction makes it impractical. The simulation experiment is carried out by using COMSOL multiphysics environment [19]. The classical method [15] is used for DOA estimation. In all of these examples, a source at a particular DOA is detected when the amplitude at that angle equals or exceeds 30% of the maximum amplitude in the spectrum. It is anticipated that $Q = 2$ to 3 harmonics will be sufficient to represent field due to scatterer and for convergence of solution because all our scatterers have radius $\rho_s \approx 0.5\lambda$ from their geometric center. It should be noted that having Q harmonics in Equation (16), will result in $2Q$ unknowns for each scatterer.

Example 1: The setup of this example is shown in Figure 2(a). Here $S = 1$ Scatterer, $L = 1$ incident plane wave and $M = 10$ Elements. The elevation of the incident wave is $\theta_1 = 60^\circ$ and scatterer (cube of side length = λ) geometric center is located at $(0.2, -0.6, 2.5)\lambda$. Figure 3(a) shows that the uncorrected DOA spectrum at $k = 0$ detects incident wave DOA $\theta_1^{(0)} = 59.4^\circ$ and two spurious DOAs 78° and 120.3°. Thus initially the algorithm has to assume three incident waves. The corrected spectrum shows error reduction for desired DOA and suppression of the spurious peaks, to the value below the 30% of the maximum value, thereby reducing the number of sources to the correct value of one. The convergence of $\theta_1^{(k)}$ to $\theta_1^{(K)} = 60.3^\circ$ using

$Q = 3$ spherical harmonics is shown in Figure 3(b).

Example 2: This example has the same geometrical setup of example 1, but has two incident plane waves $L = 2$. The elevation of the incident waves is $\theta_1 = 60°$ and $\theta_2 = 105.0°$. The algorithm initially estimates two incident waves $\theta_1^{(0)} = 58.8°$ and $\theta_2^{(0)} = 105.8°$. Two spurious DOAs 78.8° and 86.7° are also detected at $k = 0$ as shown in Figure 4. Thus initially the algorithm has to assume four incident waves. Spurious peaks in DOA spectrum are successfully reduced and DOA estimation of desired waves if reasonably achieved. The convergence of $\theta_1^{(k)}$ to $\theta_1^{(K)} = 60.3°$ and $\theta_2^{(k)}$ to $\theta_2^{(K)} = 105.2°$ using $Q = 3$ is shown in Figure 5.

Example 3: This example is more complex by not only having $S = 2$ scatterer but also closely spaced antenna elements $d = 0.25\lambda$, which causes increase in mutual coupling. The geometry is shown in Figure 2(b). The number of unknowns will increase as number of scatterers increase, so in this example more antenna elements $M = 18$ are used to provide adequate degree of freedom to the algorithm. The elevation of the incident wave $L = 1$ is $\theta_1 = 105.0°$. One scatterer in the form of cube of side length $= 0.9\lambda$ is located at $(-0.2, -0.6, 3.5)\lambda$ and the other as sphere of radius $\rho_s = 0.5\lambda$, geometric center at $(-0.2, -0.7, 0.45)\lambda$. Figure 6(a) shows that the uncorrected DOA spectrum at $k = 0$, where incident wave DOA is detected as $\theta_1^{(0)} = 103.0°$ and one spurious DOA at 129.2°. The corrected spectrum shows improved DOA estimation and snubbing of the spurious peak,

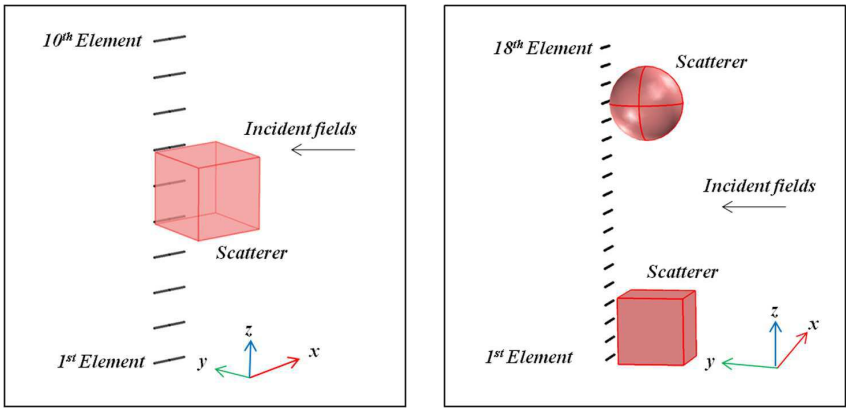

(a) (b)

Figure 2. Geometric setup for examples 1, 2, 3 & 4. (a) Antenna array and near zone scatterer for example 1 & 2. (b) Antenna array and nnear zone scatterers for example 3 & 4.

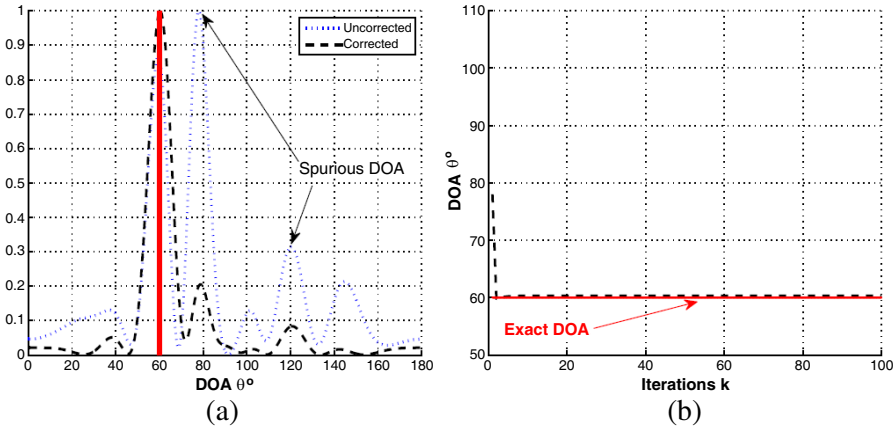

Figure 3. Results for example 1. (a) DOA spectrum for example 1. (b) Convergence of $\theta_1^{(k)}$ for example 1.

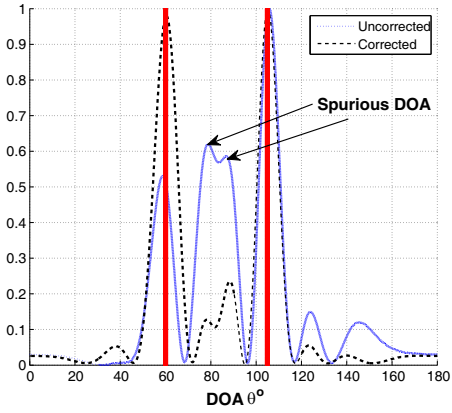

Figure 4. DOA spectrum for example 2.

thereby reducing the number of sources to the correct value of one. The convergence of $\theta_1^{(k)}$ to $\theta_1^{(K)} = 104.6°$ using $Q = 2$ spherical harmonics is shown in Figure 6(b).

Example 4: The geometrical setup of this case is same as of example 3, but has two incident plane waves $L = 2$. The elevation of the incident waves is $\theta_1 = 60°$ and $\theta_2 = 105.0°$. The algorithm initially estimates three incident waves $\theta_1^{(0)} = 61.0°$ and $\theta_2^{(0)} = 102.8°$. One spurious DOA 46.4° is also detected as shown in Figure 7. This

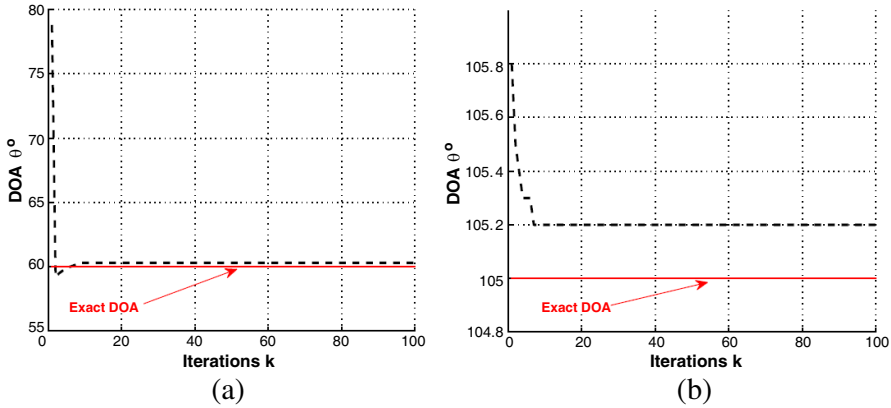

Figure 5. Convergence of $\theta_1^{(k)}$ and $\theta_2^{(k)}$ for example 2. (a) Convergence of $\theta_1^{(k)}$. (b) Convergence of $\theta_2^{(k)}$.

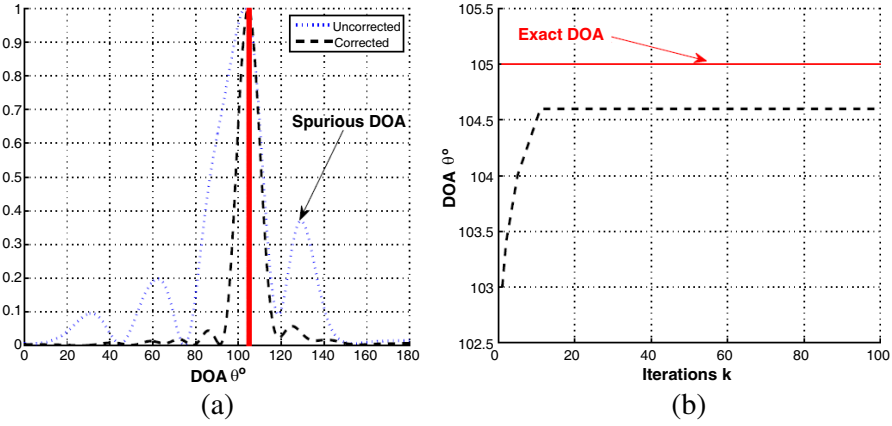

Figure 6. Results for example 3. (a) DOA spectrum for example 3. (b) Convergence of $\theta_1^{(k)}$ for example 3.

case shows the trouble an ordinary DOA estimator (un-calibrated) can face, where the spurious signal peak has almost the same value as of desired signal. Thus the spurious signal can not be rejected by setting a threshold value as this will also reject the desired signal. Oure algorithm take into account three incident waves initially. After convergence of the algorithm the unwanted signal peak is almost eradicated and DOA estimation accuracy is also improved. The

convergence of $\theta_1^{(k)}$ to $\theta_1^{(K)} = 59.4°$ and $\theta_2^{(k)}$ to $\theta_2^{(K)} = 105.4°$ using $Q = 2$ is shown in Figure 8. This example also shows the slower and erratic convergence of the solution due to the complexity of the situation. This iterative nature of the solution is a drawback of this method. From this, it is worth to mention that an approximately similar geometric situation was handled by $M = 45$ antenna elements using cylindrical harmonics [14].

The examples above demonstrated superiority of the proposed method over the one presented in [14]. First, we support our argument by having used 3D environment as against theirs 2D. Secondly, in our examples the antenna size is practical as compared to impractical very thin size proposed in the predecessor. Thirdly, we resolved DOA estimation problem with fairly lesser number of antenna elements as against them, as spherical harmonics provide better realization of scattering field. Large number of antenna elements increases hardware and cost. Another, technique presented in [11] does use spherical coordinates in resolving DOA problem in 2D, for a single near field scatterer with two incident plane waves. However as mentioned earlier, we supersede them as well by having 3D environment, multiple scatterers, and multiple incident waves. Thus, our method shows practicality and cost effectiveness. A summary of number of iterations required and convergence time using Intel®core^{TM}i5-2500 processor is given in Table 1. The number of iterations and convergence time increase as the complexity increase. However with faster processing it can be further reduced.

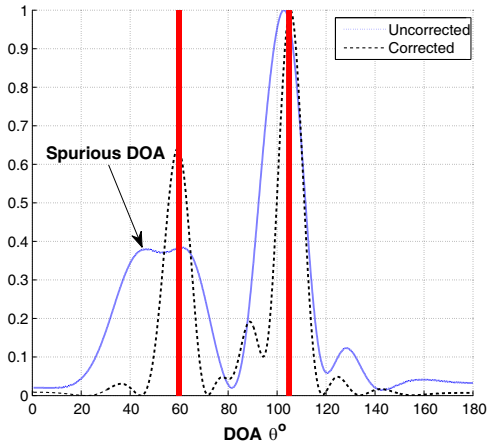

Figure 7. DOA spectrum for example 4.

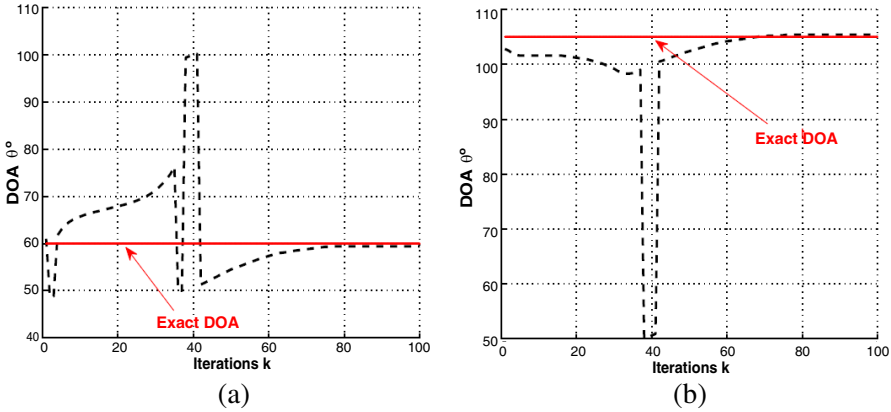

Figure 8. Convergence of $\theta_1^{(k)}$ and $\theta_2^{(k)}$ for example 4. (a) Convergence of $\theta_1^{(k)}$. (b) Convergence of $\theta_2^{(k)}$.

Table 1. Number of iterations and convergence time for examples 1–4.

Examples #	Iterations K #	Convergence time Seconds
1	10	0.33
2	10	0.33
3	12	0.392
4	78	2.23

4. CONCLUSION

The autocalibration method described here extends the state of art available in DOA estimation in the presence of near zone 3D scatterers. The work is supported by numerical examples for a variety of complex situations, in terms of multiple incident waves and scatterers. Use of spherical harmonics provides better realization of scattering field with less number of harmonics and therefore reduce the number of antenna elements required in comparison of using cylindrical harmonics. Although this approach is demonstrated to be more practical in terms of using 3D scatterers and real size antenna elements, it still carries the same two drawbacks: due to iterative method, it has limited application where time delay is acceptable and secondly as the electrical size or number of scatterers increases, the number of unknown increases, which requires more antenna elements. However, the method motivates the state of art present towards more

a realistic situation. Finding a guaranteed solution with this method is one of the open problems. Scenarios when multiple scatterers come close to each other and also to antenna elements, result in mutual coupling between scatterer-scatterer and scatterer to antenna and are yet to be addressed, to the best of our knowledge. The authors wish to continue this work for finding DOA in situations where noise is also present and the antenna and scatterer share energy.

ACKNOWLEDGMENT

The authors wish to acknowledge the the extensive contribution of Prof. Daniel R. Fuhrmann of Michigan Technological University in the preparation of this research paper.

APPENDIX A. NOMENCLATURE

B_{sq}, C_{sq}	Spherical harmonic's amplitudes
d	Element spacing in wavelength λ
E_l	Amplitudes of lth incident plane wave
E^t	Total electric field
E^{inc}	Incident electric field
E^{sct}	Scattered electric field from scatterer
f	Frequency of incident signal
$G^1_{sqm}, \ldots, G^5_{sqm}$	Spherical harmonics
$\hat{H}^{(2)}$	Spherical Hankel function of second kind
$\hat{H}^{(2)'}$	First derivative of spherical Hankel function of second kind
$\hat{H}^{(2)''}$	Second derivative of spherical Hankel function of second kind
L	Number of incident plane waves
l	Incident plane wave index
M	Number of antenna elements
m	Antenna element index
N	Number of unknowns in the set of simultaneous linear equations
P^1	Associated Legendre function of first kind
P'^1	First derivative of associated Legendre function of first kind
PW	Plane wave
Q	Number of spherical harmonics used
q	Index of spherical harmonic
r	Radial distance in spherical coordinates
r_{sm}	Radial distance from sth scatterer to mth element

S	Number of Scatterers
s	Scatterer index
U, V, W	Constants for fixed element and scatterer location
(x_m, y_m, z_m)	Location of mth antenna element in cartesian coordinates
(x_s, y_s, z_s)	Location of sth scatterer in cartesian coordinates
β	Free space wave number
θ	Elevation angle in spherical coordinates
θ_{sm}	Elevation angle of mth element from sth scatterer
(θ_l, ϕ_l)	Incidence direction of lth plane wave
ρ_a	Radius of antenna wire
ρ_s	Radius of scatterer
ϕ	Azimuth angle in spherical coordinates
ϕ_{sm}	Azimuth angle of mth element from sth scatterer

REFERENCES

1. Krim, H. and M. Viberg, "Two decades of array signal processing research: The parametric approach," *IEEE Signal Processing Magazine*, Vol. 13, No. 4, 67–94, July 1996.
2. Zhang, Y. and B. P. Ng, "Music-like DOA estimation without estimating the number of sources," *IEEE Transactions on Signal Processing*, Vol. 58, No. 3, 1668–1676, 2010.
3. Kim, K. and T. K. Sarkar, "Direction-of-arrival (DOA) estimation using a single snapshot of voltages induced in a real array operating in any environment," *Microwave and Optical Technology Letters*, Vol. 32, No. 5, 335–340, 2002.
4. Gupta, I. and A. Ksienski, "Effect of mutual coupling on the performance of adaptive arrays," *IEEE Transactions on Antennas and Propagation*, Vol. 31, No. 5, 785–791, 1983.
5. Steyskal, H. and J. S. Herd, "Mutual coupling compensation in small array antennas," *IEEE Transactions on Antennas and Propagation*, Vol. 38, No. 12, 1971–1975, 1990.
6. Friedlander, B. and A. J. Weiss, "Direction finding in the presence of mutual coupling," *IEEE Transactions on Antennas and Propagation*, Vol. 39, No. 3, 273–284, 1991.
7. Hui, H. T., "A new definition of mutual impedance for application in dipole receiving antenna arrays," *IEEE Antennas and Wireless Propagation Letters*, Vol. 3, 364–367, 2004.
8. Fabrizio, S. and S. Alberto, "A novel online mutual coupling compensation algorithm for uniform and linear arrays," *IEEE*

Transactions on Signal Processing, Vol. 55, No. 2, 560–573, 2007.

9. Zhang, Y., Q. Wan, and A.-M. Huang, "Localization of narrow band sources in the presence of mutual coupling via sparse solution finding," *Progress In Electromagnetics Research*, Vol. 86, 243–257, 2008.
10. Ye, Z. F., J. S. Dai, X. Xu, and X. P. Wu, "DOA estimation for uniform linear array with mutual coupling," *IEEE Transactions on Aerospace and Electronic Systems*, Vol. 45, No. 1, 280–288, 2009.
11. Friel, E. M. and K. M. Pasala, "Direction finding with compensation for a near field scatterer," *Antennas and Propagation Society International Symposium, APS. Digest*, Vol. 1, 106–109, 1995.
12. Burintramart, S., T. K. Sarkar, Y. Zhang, and M. Salazar-Palma, "Nonconventional least squares optimization for DOA estimation," *IEEE Transactions on Antennas and Propagation*, Vol. 55, No. 3, 707–714, 2007.
13. Henault, S. and Y. M. M. Antar, "Accurate evaluation of mutual coupling for array calibration," *Computational Electromagnetics International Workshop, CEM*, 34–37, 2009.
14. Horiki, Y. and E. H. Newman, "A self-calibration technique for a DOA array with near-zone scatterers," *IEEE Transactions on Antennas and Propagation*, Vol. 54, No. 4, 1162–1166, 2006.
15. Foutz, J., A. Spanias, and M. K. Banavar, *Narrowband Direction of Arrival Estimation for Antenna Arrays*, Morgan & Claypool Publishers, 2008.
16. Tuncer, E. and B. Friedlander, *Classical and Modern Direction-of-arrival Estimation*, Academic Press, 2009.
17. Balanis, C. A., *Advanced Engineering Electromagnetics*, Wiley, 1989.
18. Van Trees, H. L., *Detection, Estimation, and Modulation Theory: Optimum Array Processing*, Vol. IV, John Wiley and Sons, 2002.
19. Comsol multiphysics modelling and engineering simulation software, 2011.